

# **Archive ouverte UNIGE**

https://archive-ouverte.unige.ch

**Article scientifique** 

Article

1993

**Published version** 

**Open Access** 

This is the published version of the publication, made available in accordance with the publisher's policy.

Hot-carrier scattering in a metal: a ballistic-electron-emission microscopy investigation on PtSi

Niedermann, Philipp; Quattropani, Lidia; Solt, Katalin; Maggio-Aprile, Ivan; Fischer, Oystein

# How to cite

NIEDERMANN, Philipp et al. Hot-carrier scattering in a metal: a ballistic-electron-emission microscopy investigation on PtSi. In: Physical Review. B, Condensed Matter, 1993, vol. 48, n° 12, p. 8833–8839. doi: 10.1103/PhysRevB.48.8833

This publication URL: <a href="https://archive-ouverte.unige.ch/unige:117877">https://archive-ouverte.unige.ch/unige:117877</a>

Publication DOI: 10.1103/PhysRevB.48.8833

© This document is protected by copyright. Please refer to copyright holder(s) for terms of use.

# Hot-carrier scattering in a metal: A ballistic-electron-emission microscopy investigation on PtSi

# Philipp Niedermann and Lidia Quattropani

Département de Physique de la Matière Condensée, Université de Genève, CH-1211 Genève 4, Switzerland

#### Katalin Solt\*

Landis & Gyr Betriebs Corporation, Corporate Research & Development, Solid State Physics, CH-6301 Zug, Switzerland

## Ivan Maggio-Aprile and Øystein Fischer

Département de Physique de la Matière Condensée, Université de Genève, CH-1211 Genève 4, Switzerland (Received 25 January 1993; revised manuscript received 20 May 1993)

Ballistic-electron-emission microscopy (BEEM) has been used to study the PtSi/n-type Si(100) interface. Hot-electron transport has been investigated by measuring the ballistic-electron transmission as a function of position (BEEM imaging), energy (BEEM spectroscopy), and PtSi thickness (BEEM attenuation length). Hot-hole transport and electron-electron scattering have also been investigated as a function of these parameters. This study has been conducted on in situ fabricated PtSi/n-type Si(100) Schottky diodes in UHV with the silicide thickness ranging from 20 to 500 Å. The PtSi films were granular and the BEEM transmissivity was found to be homogeneous on individual grains but strongly varying from one grain to another. We attempt to compare the absolute BEEM current level with existing models and find its limiting value for small silicide thicknesses to be close to 1 depending on the model considered, indicating efficient transmission due to strong forward focusing of the electrons in the base or enhancement due to multiple scattering within the grains. BEEM current as a function of silicide thickness shows a change from a rapid to a slower decrease at about 150 Å. Reverse BEEM (RBEEM) attenuation lengths also show this qualitative behavior, but the attenuation with increasing PtSi thickness is distinctly weaker, indicating that BEEM and RBEEM intensities are differently influenced by the elastic and inelastic hot-carrier mean free paths. RBEEM spectra are found to be anomalous, indicating an anomalous distribution of the tunnel-injected hot holes in the base.

### INTRODUCTION

In ballistic-electron-emission microscopy (BEEM), hot carriers of controlled energy are injected with high spatial resolution by tunneling from a scanning tunneling microscope (STM) tip into a sample containing a subsurface electronic barrier. In the case of a Schottky barrier with an n-type semiconductor, the tip is biased negatively with respect to the metal layer ("base"). BEEM spectra are obtained by measuring the collector current in the semiconductor ("collector") as a function of tunnel voltage. This method has already been used to characterize the Schottky barrier height and its spatial homogeneity in various metal-semiconductor systems.<sup>2</sup> Biasing the tip positively, one obtains "reverse BEEM" (RBEEM) spectra by the collection of secondary hot carriers that are created via a collision process involving the initially injected carriers,<sup>3</sup> in analogy to an Auger process.

The nature of the hot-carrier transport in the BEEM experiment is subject to ongoing discussion. The initial BEEM model by Bell and Kaiser<sup>4</sup> (BK model) assumes completely ballistic carrier transport from the emitter across the base and into the collector. The component of the crystal momentum parallel to the metal-semiconductor interface ( $k_{\parallel}$ ) is assumed to be conserved which gives rise to a critical angle beyond which the electrons are totally reflected. In the BK model, any electron that is scattered in the base, elastically or inelastically, is

considered lost for collection. This is justified if the majority of the injected hot electrons are strongly forward focused and the probability is small that once scattered, an electron is scattered back into the critical angle cone. The BK model is in good agreement with the experimentally observed BEEM spectra, in particular for semiconductor interfaces where the conduction-band minimum lies at the center of the projected Brillouin zone. This is the case for Si(100)-metal interfaces, if the metal has nonzero density of states in the k-space region of interest. In contrast, the BEEM spectra observed on Au/n-type Si(111) were reported<sup>5</sup> to deviate from the prediction of the BK model for this case where the conduction-band minima lie off the center of the Brillouin zone, and it has been suggested that the electrons undergo elastic scattering in the base before entering the collector.<sup>5</sup>

The evolution of the BEEM spectral intensity with base thickness depends on the hot-carrier scattering behavior. The purpose of this paper is to examine this evolution in a large range of thicknesses from 20 to 500 Å. We have found that the thickness dependences of the BEEM and reverse BEEM intensities are different. In our interpretation, this is due to a different influence of the elastic and the inelastic electron mean free path (MFP's) on the attenuation lengths of the two physical processes. We confirm that the RBEEM intensity is higher than expected<sup>3</sup> and also report an anomalous spectral shape. These as yet unexplained effects raise questions on the spectral distribution of the injected hot holes.

#### **EXPERIMENT**

Si(100) substrates (5  $\Omega$  cm), back implanted for Ohmic contacts, were thermally oxidized to 1300 Å of SiO<sub>2</sub> and etched in HF:methanol 1:4 to prepare clean hydrogenterminated surfaces,6 rinsed in methanol, and introduced into UHV within 4 min. After this, all preparation steps and the BEEM measurements were performed in situ. The cleanliness of the Si surfaces was verified with Auger electron spectroscopy (AES) and the residual contamination was estimated to be ≈0.05 monolayers of O and ≈0.15 monolayers of C showing the Si surface to be hydrogen terminated; no Si peak component characteristic of  $SiO_x$  was detected. Platinum was dc magnetron sputter deposited at a pressure of 0.2 mbar Ar (99.9999% purity), at a rate of 0.6 Å/s and at a base pressure of  $5 \times 10^{-9}$  mbar. The thickness of the deposited Pt was calibrated by stylus profilometry. A shadow mask was used to define the diode area of  $\approx 0.29 \text{ mm}^2$ . The mask was then removed and the PtSi was formed by heating to 500 °C for 30 min. The resulting silicide had a surface contamination of about one monolayer of C and O; no bulk or interface contamination was detected by AES depth profiling. Auger electron spectroscopy revealed the ratio of Pt to Si peak intensities to be independent of silicide thickness, suggesting that the PtSi was fully formed for all thicknesses studied.<sup>7</sup> The impedance of these Schottky diodes was on the order of 10 M  $\Omega$ , allowing low-noise BEEM measurements with a favorable signal-to-noise ratio.

For the BEEM measurements, samples were transferred in UHV to the surface analysis-STM chamber with a base pressure in the low 10<sup>-11</sup>-mbar range. We used a home-built UHV STM that was designed to position the tip above any point on a 1-cm<sup>2</sup> surface under scanning electron microscope control.<sup>8</sup> Gold tips were used for these measurements.

### THEORY

An important part of the experimental results that will be presented are the absolute spectral intensities. We define the intensity of a BEEM spectrum in terms of the collector current level just above threshold. The onset is close to quadratic, in analogy to the Fowler law of photoemission which is a similar physical process. A correction due to quantum-mechanical reflection at the interface is expected to give rise to a  $\frac{5}{2}$  power law at onset but will be neglected here. In order to discuss BEEM and RBEEM intensities quantitatively, we develop approximations for the collector current versus tunnel voltage in this section.

In the widely used BK model for BEEM,<sup>4</sup> the collector current  $I_{c,BK}$  is the fraction of the tunnel current between tip and base that is ballistically transmitted across the base and into electronic states in the semiconductor; see Fig. 1. It is given as the integral over the tunnel barrier transmission coefficient  $D(E_{\perp})$  over the normal and parallel (to the interface) kinetic energies in the tip,  $E_{\perp}$  and  $E_{\parallel}$ ,

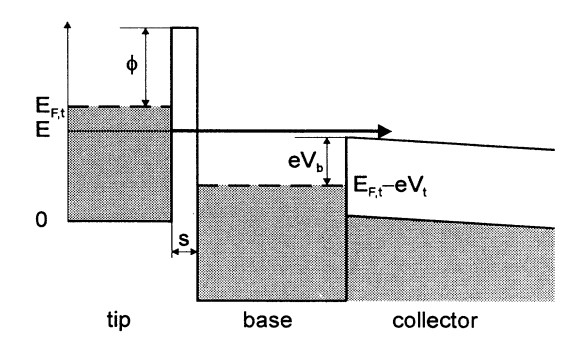


FIG. 1. Band diagram of the BEEM experiment.

$$I_{c,\mathrm{BK}} = ARC \int_{E_{\mathrm{min}}}^{\infty} dE_{\perp} D(E_{\perp}) \int_{0}^{E_{\mathrm{max}}} dE_{\parallel} f(E) , \qquad (1)$$

where  $C=2em/[(2\pi)^2\hbar^3]$ , and  $E_{\min}=E_{F,t}-e(|V_t|-V_b)$  represents the minimum normal energy necessary for the electrons to cross the metal-semiconductor barrier of height  $V_b$ .  $V_t$  is the tip bias and  $E_{F,t}$  is the Fermi level in the tip.  $E_{\max}=[m_t/(m-m_t)]\times[E_1-E_{F,t}+e(|V_t|-V_b)]$  is the maximum parallel energy in the tip for which an electronic state in the semiconductor is available that fulfills energy and  $\mathbf{k}_{\parallel}$  conservation. m is the free-electron mass and  $m_t$  the transverse electron mass in the semiconductor. f(E) is the Fermi function in the tip, with  $E=E_1+E_{\parallel}$ . A is the area and R is a scale factor, representing the probability that an electron can reach the interface ballistically. Here and in the following, free-electron energy dispersions are assumed for tip and base. The tunnel current between tip and base is given by a similar integral,

$$I_{t} = AC \int_{0}^{\infty} dE_{\perp} D(E_{\perp}) \int_{0}^{\infty} dE_{\parallel} [f(E) - f(E + e |V_{t}|)] . \tag{2}$$

Writing  $\underline{D}(E_{\perp}) \approx D(E_{F,t}) \exp[-\beta(E_{F,t} - E_{\perp})/2\sqrt{\phi}]$ , with  $\beta = 2\sqrt{2m}s/\hbar$  and  $\phi$  the height and s the width of the vacuum barrier, we can write approximately for large  $|V_t|$ ,

$$I_t = ACD(E_{F,t})4\phi/\beta^2. \tag{3}$$

Here and in the following, we use the zero-temperature limit. For  $|V_t|$  just above the Schottky barrier height  $V_b$ , i.e., for  $e(|V_t|-V_b) \ll 2\sqrt{\phi}/\beta$  so that  $D(E_\perp) \approx D(E_{F,t})$ , we can write  $I_c$  to first order as  $ARCD(E_{F,t})e^2(|V_t|-V_b)^2m_t/2m$ , representing the well-known quadratic onset of the collector current, and dividing this expression by (3) we obtain

$$I_{c, BK} \approx R \frac{m_t e^2 s^2}{\hbar^2 \phi} (|V_t| - V_b)^2 I_t$$
 (4)

The quadratic onset is a general property of any emission of electrons with a constant density below a maximum energy into a medium with a parabolic band minimum. In Eq. (4), we see that for a given spectrum, the intensity depends on the width and height of the tunnel barrier. This reflects the fact that for a wide barrier, the tunneling

electrons are more sharply forward focused and also that their density decreases more rapidly with decreasing  $E_{\perp}$ .

A different view of the transmission process has been proposed recently by Lee and Schowalter<sup>10</sup> (LS model) who assumed that the hot-electron velocities are completely randomized in the base due to elastic scattering. In this case,  $I_c$  is given as follows:

$$I_{c,\mathrm{LS}} = ARC \int \int dE_{\parallel} dE_{\perp} f(E) 0.5 [1 - \cos\theta_c(E)] D(E_{\perp}) , \qquad (5)$$

where the domain of the integral is given by  $E > E_{F,t} - e(|V_t| - V_b)$ , the condition that only electrons with energy above the Schottky barrier maximum can be transmitted. We do not, however, include here the effect of pair creation in the semiconductor that LS also include in their model.  $\theta_c(E)$  is the critical angle in the base for electron collection and is given by

$$\sin^2 \theta_c = \frac{m_t}{m} \frac{E + e(|V_t| - V_b) - E_{F,t}}{E + e|V_t|} \ . \tag{6}$$

Naturally, the onset again follows a quadratic law. Using the same approximation for  $D(E_{\perp})$  and integrating over E and  $E_{\perp}$  we find an approximate expression,

$$I_{c, \rm LS} \approx R \frac{m_t e^2 s}{4 \sqrt{2m} \, \hslash (eV_b + E_{E,t}) \sqrt{\phi}} (|V_t| - V_b)^2 I_t \ .$$
 (7)

Comparing Eqs. (4) and (7), we find that for typical values of  $\phi$  and s,  $I_{c,LS}$  is much lower than  $I_{c,BK}$ ; taking, for example,  $\phi = 2$  eV, s = 6.0 Å, and  $E_{f,t} = 5.5$  eV, we have  $I_{c,BK}/I_{c,LS} = 56$ . This is not unexpected, since a widening up of the electron distribution necessarily reduces the probability for the electrons to enter the semiconductor.

As already mentioned, applying a positive voltage to the tip also gives rise to a collector current and RBEEM spectra can be measured.<sup>3</sup> In this process (Fig. 2), hot holes are created in the base by tunneling of electrons to the tip. The holes are filled by electron-hole collisions with the maximum energy gain given by the tip voltage. This energy is transferred to another electron, up to a maximum kinetic energy in the base of  $E_{F,b} + eV_t$ . If  $V_t > V_b$ , electrons may enter the semiconductor, creating a collector current of the same sign as the direct BEEM current. It has been shown experimentally<sup>3</sup> that the onset of the RBEEM occurs at the same absolute value of

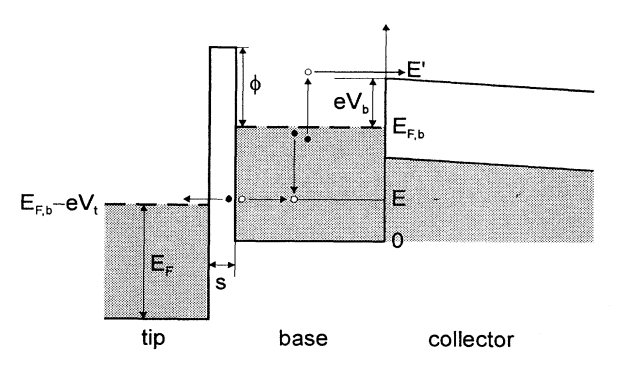


FIG. 2. Band diagram of the RBEEM experiment.

the tunnel voltage as the onset of the direct BEEM.

Assuming again free electrons and zero temperature, this collector current can be calculated as

$$I_{c,R} = AC \int_{E_{F,b}-V_t}^{E_{F,b}} dE \int_0^E dE_{\perp} P(E, E_{\perp}) D(E_{\perp}) ,$$
 (8)

taking kinetic energies in the base, where  $E_{F,b}$  is the Fermi energy in the base.  $P(E,E_{\perp})$  is the probability that a hot hole with kinetic energy E decays in the manner described above and creates a hot electron with energy above  $eV_b$  and with its k vector within the critical angle of collection. We will now derive approximate expressions for  $P(E,E_{\perp})$  and  $I_{c,R}$  based on the model of Bell  $et\ al.$  Assuming that the hot holes lose energy exclusively via this scattering process, and excluding multiple scattering,  $P(E,E_{\perp})$  is given by

$$P(E, E_{\perp}) = \sum_{\mathbf{k}': \theta < \theta_{c}} R(\mathbf{k}, \mathbf{k}') / \sum_{\mathbf{k}'} R(\mathbf{k}, \mathbf{k}') , \qquad (9)$$

where  $\theta$  is the angle of  $\mathbf{k}'$  with the interface plane and  $R(\mathbf{k}, \mathbf{k}')$  is the transition rate from an initial state with crystal momentum  $\mathbf{k}$  to a final state with  $\mathbf{k}'$  [assuming free-electron energy dispersions  $E(\mathbf{k})$ ,  $E'(\mathbf{k}')$ , and  $E_{\perp}(\mathbf{k}_{\perp})$ ] and is given as 11

$$R(\mathbf{k},\mathbf{k}') = \operatorname{const} \times \frac{2E_{F,b} - E - E'}{(E + E' + 2\sqrt{EE'}\cos\alpha)^{1/2}}, \quad (10)$$

with  $\alpha$  the angle between **k** and **k'**. Since  $E \ll E'$  (and because there may be a tendency toward isotropic distribution of the hot holes due to elastic scattering and specular reflection), we replace  $R(\mathbf{k}, \mathbf{k'})$  by its angular average

$$R(k,k') = \operatorname{const} \times \frac{2E_{F,b} - E - E'}{\sqrt{E}} . \tag{11}$$

To first order, we then obtain an isotropic expression for the scattered electron collection probability,

$$P(E, E_{\perp}) \approx P(E) = \frac{m_t}{6m} \frac{(E_{F,b} - eV_b - E)^3}{(E_{F,b} + eV_b)(E_{F,b} - E)^2} . \tag{12}$$

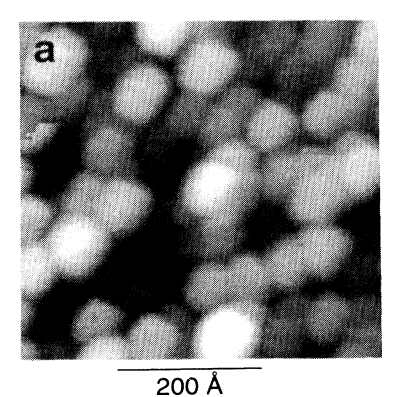
The slow onset of P(E) for  $E < E_{F,b} - eV_b$  comes from the fact that the hot-electron distribution tails off to zero at its maximum energy  $E' = 2E_{F,b} - E$ . Using Eqs. (3) and (8), we obtain an approximation for the collector current in RBEEM,

$$\frac{I_{c,R}}{I_t} \approx \exp(-\beta \left[\sqrt{\phi + eV_b} - \sqrt{\phi}\right]) \times \frac{\beta \sqrt{\phi + eV_b}}{\phi} \frac{m_t}{48m} \frac{(eV_t - eV_b)^4}{(E_{E,b} + eV_b)(eV_b)^2} .$$
(13)

As we will show with a specific example, this approximation is only good for a relatively small energy interval above threshold, due to the rapid decrease of the tunneling probability with decreasing E.

# RESULTS AND DISCUSSION

Typically, the silicide films had a granular appearance with grain sizes of  $\approx 100$  Å as shown in a representative



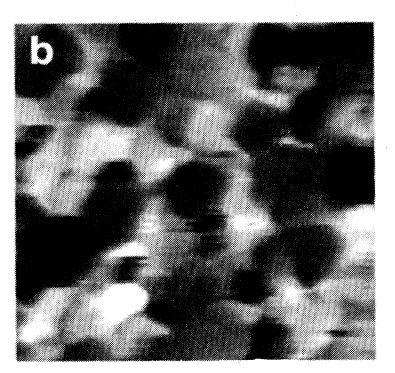


FIG. 3. (a) Topographic image and (b) simultaneously measured collector current image for a sample with  $d_{\rm PiSi}$  = 40 Å. Gray scales are 40 Å and 57 pA, respectively.  $V_t$  = -1.5 V,  $I_t$  = 1 nA.

STM image in Fig. 3(a). The rms roughness was found to be practically independent of  $d_{\text{PtSi}}$  at  $\approx 8 \text{ Å}$  which is close to the rms roughness of  $\approx 6$  Å of our Si substrates. A comparison with the simultaneously measured collector current [Fig. 3(b)] reveals a striking behavior. Very typically for our silicides, the collector current is strongly correlated with the grain morphology, very homogeneous on an individual grain but with the intensity varying strongly from one grain to another; drops of  $I_c$  by more than a factor of 50 were not unusual. This large contrast may reflect different crystalline orientations of the grains, in agreement with TEM investigations on PtSi overlayers. 12 We note that we do not observe a correlation of the BEEM intensity with the slope of the surface, as could be expected due to the critical angle for electron transmission across the interface ("searchlight effect").9

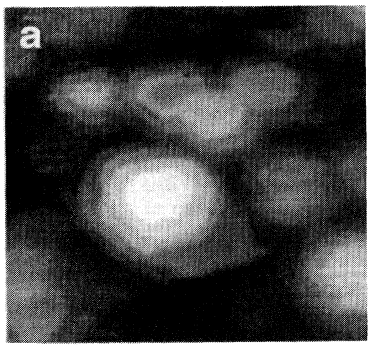
An example where STM showed the PtSi layer to be crystalline is given in the topograph in Fig. 4(a). Such evidence of crystallinity as observed occasionally on our samples, indicating that the films tended to grow with local epitaxy. The observed step height of  $\approx 4$  Å corresponds to the crystal lattice plane separation of a known<sup>12</sup> (110) epitaxial orientation of PtSi on Si(100). In these images, the collector current intensity was again strongly correlated with grain morphology.

In order to study barrier heights and to determine average intensities, BEEM and RBEEM spectra were acquired over an area of  $5\times5~\mu m$ , at positions spaced 5000 Å apart, which is on the order of the Debye length of the

substrate. At each position, a spectrum was acquired by averaging over 50 voltage sweeps including both polarities, each sweep taking about 2 s.

Within measuring precision, the Schottky barrier height  $V_b$  obtained from fits with BK theory, Eq. (1), was found to be independent of position for a given silicide thickness. For  $d_{\text{PtSi}} = 20$  Å, we found  $V_b = 0.87 \pm 0.02$  V; with increasing thickness,  $V_b$  decreased gradually to  $0.81 \pm 0.03$  V at  $d_{\text{PtSi}} = 200$  Å, similar to what we had observed earlier on ex situ prepared PtSi/Si(100) diodes and to what has been reported in literature. The observed homogeneity of  $V_b$  does not, however, rule out Schottky barrier height variations on a scale much smaller than the Debye length.

Turning to BEEM spectroscopy, we compare in Fig. 5 an averaged spectrum for  $d_{PtSi} = 120 \text{ Å}$  with the two BEEM models discussed above, the BK model, Eq. (1), and the LS model, Eq. (5). For the purpose of this comparison, the data are fitted with a square law in a region where  $dI_c/dV$  is linear, thus determining  $V_b$ . The model curves are rescaled to fit the data for  $|V_t| < 1.2 \text{ V}$ . We note that the derivative BK mode spectrum shows a stronger rollover with increasing voltage<sup>15</sup> than the experimental curve while the LS model appears to fit the data better up to  $\approx 1.3 \text{ V}$ . Taking the full LS theory<sup>10</sup> (i.e., including pair creation in the semiconductor) may lead to a better fit at higher energies although our rollover appears to occur at an energy which is higher than the Si band gap. These are very subtle differences, not





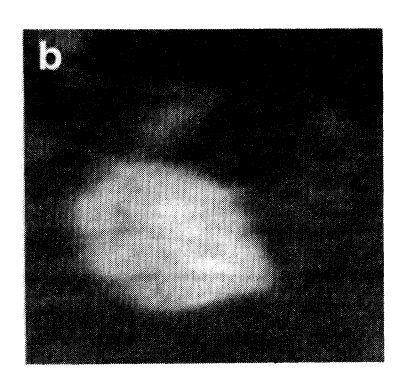


FIG. 4. (a) Topographic image and (b) simultaneously measured collector current image for a sample with  $d_{PtSi} = 50 \text{ Å}$  which had crystalline appearance. Gray scales are 25 Å and 30 pA, respectively.  $V_t = -1.5 \text{ V}$ ,  $I_t = 1 \text{ nA}$ .

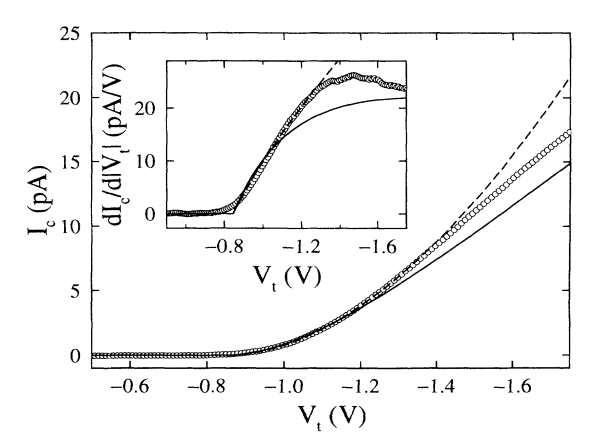


FIG. 5. BEEM spectrum (circles) and derivative (inset) for a sample with  $d_{\text{PtSi}} = 120 \text{ Å}$  with a comparison with the BK model, Eq. (1), solid line, and the LS model, Eq. (5), dashed line. The intensities of the model curves are adjusted to fit the data for  $|V_t| < 1.2 \text{ V}$  by scaling them with R = 0.020 and 0.82, respectively, using  $\phi = 2 \text{ eV}$  and s = 6.0 Å. Tunnel current was 5 nA;  $V_b$  from the fit is 0.85 V.

apt to discriminate between the models, given the complex system that we are investigating. Finally, we note that the slightly too low  $V_b$  together with the low-energy tail may indicate the presence of a thin n<sup>+</sup>-doped layer at the interface. <sup>16</sup>

Figure 6 shows the PtSi thickness dependence of the BEEM intensity near onset as determined from fits with the parabolic law  $I_c = I_t B (|V_t| - V_b)^2$ . Compared with our earlier results on ex situ PtSi/Si(100) diodes, <sup>13</sup> the intensities are about one order of magnitude higher (showing that an oxygen-rich top layer that is invariably present on ex situ PtSi samples reduces hot-electron transmission besides inducing variations in the onset of the spectra). Also indicated in Fig. 6 are the intensities predicted by the two discussed models for the case of lossless transmission (R=1). We observe that an inter-

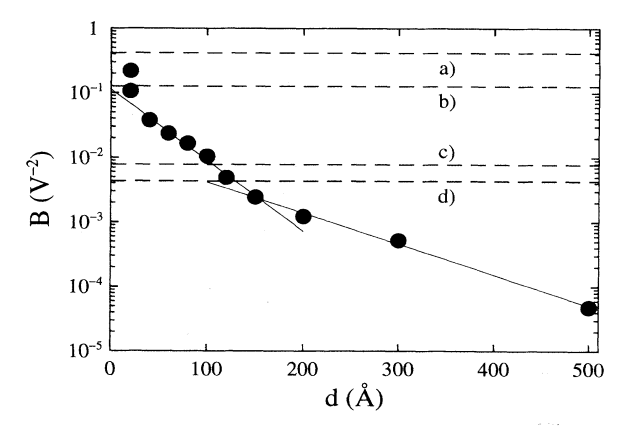


FIG. 6. Logarithmic average of the BEEM spectral intensity vs PtSi thickness from fits to the parabolic law  $I_c = I_t B (|V_t| - V_b)^2$  for  $|V_t| \le 1.2$  V. The dashed lines indicate the levels for "ideal transmission" (R=1) for the BK model, Eq. (4), for (a)  $\phi = 2$  eV, s = 5.7 Å and (b)  $\phi = 4$  eV, s = 4.5 Å and for the LS model, Eq. (7), for (c)  $\phi = 2$  eV, s = 5.7 Å and (d)  $\phi = 4$  eV, s = 4.5 Å. Solid lines correspond to  $B \sim \exp(-d_{PtSi}/\lambda)$  with  $\lambda = 40$  and 91 Å.

pretation in terms of the BK model (lines a and b) results in R < 1 for all thicknesses if a work function on the order of 2 eV is assumed whereas within the LS model (lines c and d), the transmission probability R is larger than 1 for the thinner layers.

There are several physical effects which may influence the absolute intensity and comparisons with the models must be exercised with caution. On the one hand, multiple reflections at interface and surface tend to increase the electron collection efficiency. On the other hand, quantum-mechanical reflection at the interface tends to decrease the transmission probability, and so does elastic or inelastic scattering at the surface. Our data show that the transmission is strong for small thicknesses in terms of both models. This seems to indicate that electrons are strongly forward focused as in the BK model, but it is also conceivable that elastic scattering of the electrons in the base is strong and that the high intensity is due to much enhanced collection efficiency through multiple scattering at interface and surface.

From Monte Carlo simulations, 5,17 hot-electron attenuation in a metal is expected to be approximately exponential. In contrast to this, we observe (Fig. 6) that the decrease of the logarithm of B with thickness comprises two linear regions; the initial decrease is described approximately by  $I_c \sim \exp(-d_{PtSi}/40 \text{ Å})$ , and for thicknesses above  $\sim 150 \text{ Å}$ , the decrease is less pronounced with  $I_c \sim \exp(-d_{PtSi}/91 \text{ Å})$ . This may reflect a bilayer nature of the thicker silicide films, with an elastic MFP of  $\approx 40$  Å for one layer and  $\approx 91$  Å for the other layer. This bilayer nature is speculative; it may, for example, be due to the systematic presence (for example, in a region near the interface not thicker than 150 Å) of dislocations, defects, or slight compositional differences below detection limit of Auger electron spectroscopy.<sup>17</sup> The study of RBEEM spectra and intensities provides us with an additional powerful tool to explore hot-carrier behavior. Figure 7 shows an RBEEM spectrum for  $d_{\text{PtSi}} = 20 \text{ Å}$ , obtained by averaging a series of spectra. Owing to the slow onset and the low currents, we can only give an upper limit for the onset of the spectrum; a significant collector current was only observed above ~1.1 V. Figure 7 also shows a fit to the fourth power approximation, Eq. (13) and a comparison with Eq. (8), numerically evaluated using the isotropic collection probability P(E). [Using the anisotropic  $P(E, E_{\perp})$  numerically calculated from Eq. (9) gives a very similar result.] Surprisingly, the agreement is very good for the approximate formula but less satisfactory for Eq. (8) which should actually be more exact. As mentioned before, Eq. (13) is a good approximation of Eq. (8) only closely above threshold. At higher energies, the curves deviate strongly from one another, due to the exponential nature of the tunneling transmission coefficient  $D(E_1)$ . This unexpected spectral behavior and the fact that the RBEEM current is higher than expected as has been reported before<sup>3</sup> both point to an anomalous hot-hole distribution in the base. The hot-hole density appears to decrease less strongly with energy than predicted from the electrontunneling process across the vacuum barrier.

The RBEEM intensity vs PtSi thickness is shown in

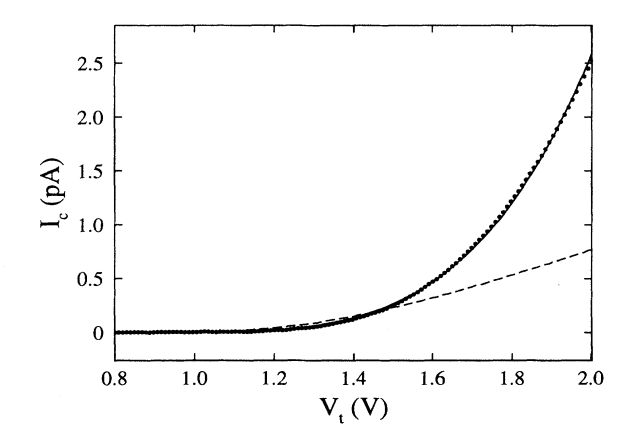


FIG. 7. RBEEM spectrum (circles) for a sample with  $d_{\text{PtSi}} = 20 \text{ Å}$  and  $I_t = 1 \text{ nA}$  together with the fourth power law according to Eq. (13) (solid line), multiplied by 2.0 to fit the experimental curve and a numerically calculated curve (dashed line) according to Eqs. (8) and (11) (see text), also multiplied by 2.0, both for  $V_b = 0.85 \text{ V}$ .

Fig. 8. This intensity decreases less strongly with increasing  $d_{PtSi}$  than does the direct BEEM intensity. The difference was also clearly visible in the individual spectra as the ratio between the reverse and direct intensities changed with  $d_{PtSi}$ . A qualitative explanation of this behavior might be that in RBEEM, the excited hot electrons in the base are expected to have a nearly isotropic distribution, unlike the injected electrons in direct BEEM. It is therefore natural to assume that the  $I_{c,R}$  vs  $d_{\text{PtSi}}$  dependence is governed by the attenuation length<sup>17</sup> L, i.e., the diffusion length for inelastic collisions rather than the elastic MFP. The attenuation length is the net distance a carrier can travel without undergoing a high energy loss (electron-electron) scattering event while its trajectory is a random walk due to (quasi)elastic collisions. That the characteristic length is the attenuation length may be plausible if one assumes, as in Refs. 3 and 11, that all hot holes decay by the electron-electron scattering channel, and that the loss of intensity occurs due to scattering of the hot electrons before they can enter the semiconductor. However, other intensity reducing mechanisms may also be significant such as hot holes entering the valence band of the semiconductor and losing energy there, hot holes or electrons losing energy by optical-phonon collisions, or hot carriers decaying radiatively by interband transitions. But the high intensity of the RBEEM signal seems to indicate that these effects are not very strong in the present case.

As for the direct BEEM, the RBEEM intensity vs  $d_{\text{PtSi}}$  plot shows two regions. Assigning the slope of the logarithmic  $I_c$  vs  $d_{\text{PtSi}}$  plot to the attenuation length L, we find  $L \approx 46$  Å for  $d_{\text{PtSi}} < 150$  Å and  $L \approx 174$  Å for the thicker layers. If our interpretation is correct, then we have a bilayer structure with one layer where both elastic and inelastic MFP's are short, with the latter barely longer than the former, and another layer with larger MFP's and the inelastic MFP significantly larger than the

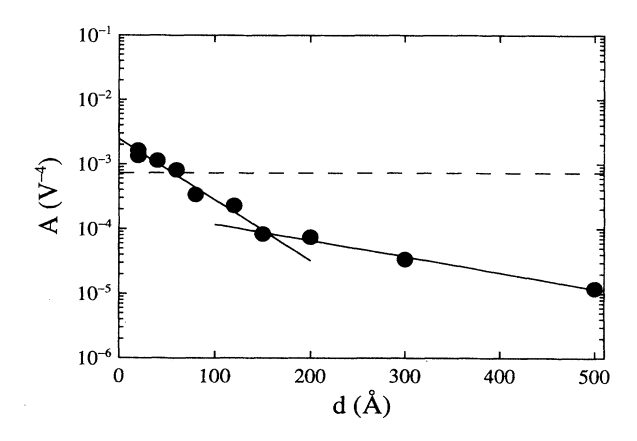


FIG. 8. Logarithmic average of the RBEEM spectral intensity vs PtSi thickness, from fits to the fourth power law  $I_c = I_t A (V_t - V_b)^4$  in the voltage interval from 0.5 to 2 V. The dashed line indicates the level of intensity predicted by Eq. (13) for  $\phi = 2$  eV and s = 5.7 Å. Lines correspond to  $A \sim \exp(-d_{PtSi}/\lambda)$  with  $\lambda = 46$  and 174 Å.

elastic one. These results are thought to give a qualitative trend; a precise quantitative determination of L would require a more detailed knowledge of the angular distribution of the elastic-scattering events.

In summary, we have performed a detailed study of direct BEEM and reverse BEEM on PtSi, and in particular of the detailed spectral shapes and the intensities vs silicide thickness from 20 to 500 Å. Our principal findings can be summarized as follows.

(i) The BEEM transmission process is an efficient one; the high BEEM intensity for thin base layers indicates that the hot electrons in the base are either strongly forward focused or are able to make multiple attempts to enter the semiconductor due to multiple scattering at the metal-vacuum and the metal-semiconductor interfaces. The interface transmission probability appears to be strongly dependent on grain orientation.

(ii) Spectral shapes deviate from the standard models for BEEM and in particular for RBEEM. This is indicative of a modified hot-carrier distribution in the base, particularly for RBEEM; this distribution appears to be less dependent of energy than expected.

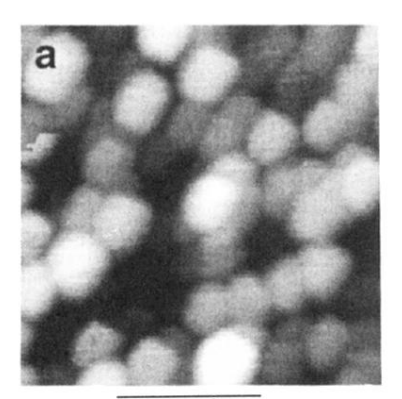
(iii) BEEM and RBEEM intensities deviate from a simple exponential dependence on thickness. Tentatively, this can be attributed to a bilayer structure for the thicker films. These appear composed of a layer with relatively short elastic mean free path and attenuation length ( $\approx$ 40 and 46 Å) and a layer where these quantities are larger ( $\approx$ 91 and 174 Å).

### **ACKNOWLEDGMENTS**

It is a pleasure to thank M. H. Hecht, L. D. Bell, and W. J. Kaiser of the Jet Propulsion Laboratory for numerous helpful discussions. We would like to acknowledge the efficient technical assistance of J.-G. Bosch and the high quality work of the mechanical workshop of the University of Geneva.

- \*Present address: Eidgenössische Technische Hochschule, Institute for Quantum Electronics-HPT, CH-8093 Zürich, Switzerland.
- <sup>1</sup>W. J. Kaiser and L. D. Bell, Phys. Rev. Lett. **60**, 1406 (1988).
- <sup>2</sup>For example, M. H. Hecht, L. D. Bell, W. J. Kaiser, and F. J. Grunthaner, Appl. Phys. Lett. **55**, 780 (1989); R. Ludeke, M. Prietsch, and A. Samsavar, J. Vac. Sci. Technol. B **9**, 2342 (1991); T.-H. Shen, M. Elliot, A. E. Fowell, A. Cafolla, B. E. Richardson, D. Westwood, and R. H. Williams, *ibid.* **9**, 2219 (1991); W. J. Kaiser, M. H. Hecht, R. W. Fathauer, L. D. Bell, E. Y. Lee, and L. C. Davis, Phys. Rev. B **44**, 6546 (1991); Y. Hasegawa, Y. Kuk, R. T. Tung, P. J. Silverman, and T. Sakurai, J. Vac. Sci. Technol. B **9**, 578 (1991); H. D. Hallen, A. Fernandez, T. Huang, R. A. Buhrman, and J. Silcox, *ibid.* **9**, 585 (1991).
- <sup>3</sup>L. D. Bell, M. H. Hecht, W. J. Kaiser, and L. C. Davis, Phys. Rev. Lett. **64**, 2679 (1990).
- <sup>4</sup>L. D. Bell and W. J. Kaiser, Phys. Rev. Lett. **61**, 2368 (1988).
- <sup>5</sup>L. J. Schowalter and E. Y. Lee, Phys. Rev. B 43, 9308 (1991).
- <sup>6</sup>P. O. Hahn, J. Vac. Sci. Technol. A 2, 574 (1984).
- <sup>7</sup>K. Solt, Vacuum **38**, 703 (1988).
- <sup>8</sup>R. Emch, Ph. Niedermann, P. Descouts, and Ø. Fischer, J. Vac. Sci. Technol. A 6, 379 (1988).

- <sup>9</sup>M. Prietsch and R. Ludeke, Phys. Rev. Lett. **66**, 2511 (1991).
- <sup>10</sup>E. Y. Lee and L. J. Schowalter, Phys. Rev. B **45**, 6325 (1992).
- <sup>11</sup>L. D. Bell, W. J. Kaiser, M. H. Hecht, and L. C. Davis, J. Vac. Sci. Technol. B 9, 594 (1991).
- <sup>12</sup>H. Ben Ghozlene, P. Beaufrère, and A. Authier, J. Appl. Phys. 49, 3998 (1978).
- <sup>13</sup>Ph. Niedermann, L. Quattropani, K. Solt, A. D. Kent, and Ø. Fischer, J. Vac. Sci. Technol. B 10, 580 (1992).
- <sup>14</sup>M. Wittmer, Phys. Rev. B 43, 4385 (1991); J. Silverman, P. Pellegrini, J. Comer, A. Golvbovic, M. Weeks, J. Mooney, and J. Fitzgerald, in *Thin Films—Interfaces and Phenomena*, edited by R. J. Nemanich, P. S. Ho, and S. S. Lau, MRS Symposia Proceedings No. 54 (Materials Research Society, Pittsburgh, 1986), p. 515.
- <sup>15</sup>The rollover of the BK spectra is a general prediction of this model although the detailed behavior depends on the height and width of the tunnel junction. Varying  $\phi$  between 0.5 and 5 eV and s between 5 and 15 Å does not markedly improve the agreement with the experimental spectra.
- <sup>16</sup>L. Quattropani, K. Solt, Ph. Niedermann, I. Maggio-Aprile, Ø. Fischer, and T. Pavelka, Appl. Surf. Sci. 70/71, 391 (1993).
- <sup>17</sup>R. N. Stuart, F. Wooten, and W. E. Spicer, Phys. Rev. Lett. 10, 7 (1963).



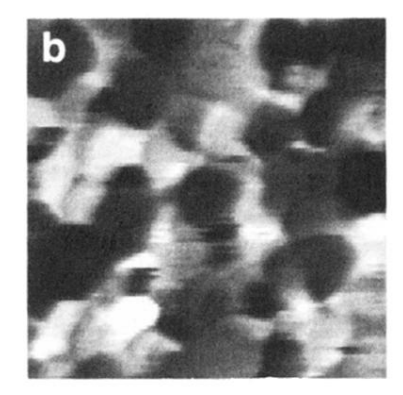
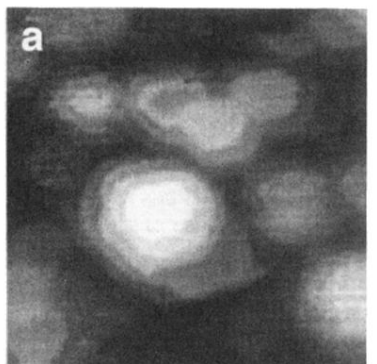
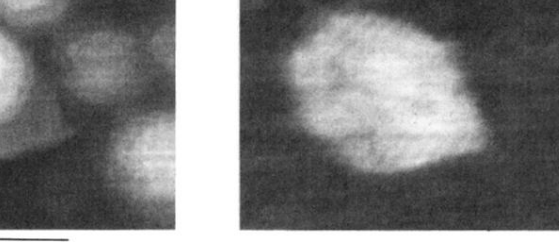


FIG. 3. (a) Topographic image and (b) simultaneously measured collector current image for a sample with  $d_{\rm PtSi} = 40$  Å. Gray scales are 40 Å and 57 pA, respectively.  $V_t = -1.5$  V,  $I_t = 1$  nA.

200 Å





b

FIG. 4. (a) Topographic image and (b) simultaneously measured collector current image for a sample with  $d_{PtSi} = 50 \text{ Å}$  which had crystalline appearance. Gray scales are 25 Å and 30 pA, respectively.  $V_t = -1.5 \text{ V}$ ,  $I_t = 1 \text{ nA}$ .

200 Å